American Mineralogist, Volume 97, pages 592–597, 2012

Electronic spin states of ferric and ferrous iron in the lower-mantle silicate perovskite

Jung-Fu Lin,[1,*] Ercan E. Alp,[2] Zhu Mao,[1] Toru Inoue,[3] Catherine McCammon,[4] Yuming Xiao,[5] Paul Chow,[5] and Jiyong Zhao[2]

[1]Department of Geological Sciences, Jackson School of Geosciences, The University of Texas at Austin, Austin, Texas 78712, U.S.A.
[2]Advanced Photon Source, Argonne National Laboratory, Argonne, Illinois 60439, U.S.A.
[3]Geodynamics Research Center, Ehime University, Matsuyama 790-8577, Japan
[4]Bayerisches Geoinstitut, Universität Bayreuth, D-95440 Bayreuth, Germany
[5]HPCAT, Geophysical Laboratory, Carnegie Institution of Washington, Argonne, Illinois 60439, U.S.A.

Abstract

The electronic spin and valence states of iron in lower-mantle silicate perovskite have been previously investigated at high pressures using various experimental and theoretical techniques. However, experimental results and their interpretation remain highly debated. Here we have studied a well-characterized silicate perovskite starting sample [$(Mg_{0.9},Fe_{0.1})SiO_3$] in a chemically inert Ne pressure medium at pressures up to 120 GPa using synchrotron Mössbauer spectra. Analyses of the Mössbauer spectra explicitly show a high-spin to low-spin transition of the octahedral-site Fe^{3+} occurring at ~13–24 GPa, as evidenced from a significant increase in the hyperfine quadrupole splitting. Two quadrupole doublets of the A-site Fe^{2+}, with extremely high-QS values of 4.1 and 3.1 mm/s, occur simultaneously with the spin transition of the octahedral-site Fe^{3+} and continue to develop to 120 GPa. It is conceivable that the spin-pairing transition of the octahedral-site Fe^{3+} causes a volume reduction and a change in the local atomic-site configurations that result in a significant increase of the quadrupole splitting in the dodecahedral-site Fe^{2+} at 13–24 GPa. Our results here provide a coherent explanation for recent experimental and theoretical results on the spin and valence states of iron in perovskite, and assist in comprehending the effects of the spin and valence states of iron on the properties of the lower-mantle minerals.

Keywords: Silicate perovskite, diamond-anvil cell, spin transition, lower mantle, synchrotron Mössbauer spectroscopy, high pressures

Introduction

Magnesium silicate perovskite ($MgSiO_3$), with 5–10 mol% Fe and Al, is the most abundant silicate phase in Earth's lower mantle, existing from 660 km in depth to several hundred kilometers above the core-mantle boundary (Ringwood 1982). The presence of the transition-metal iron in lower-mantle perovskite can affect a broad spectrum of the material's physical and chemical properties; thus, knowing the exact electronic spin and valence states of iron in perovskite at relevant pressure-temperature conditions is of great interest to deep-Earth research (e.g., see reviews by McCammon 1997, 2006; Li 2007; Lin and Tsuchiya 2008). Previous experimental and theoretical studies suggest that iron in perovskite exists in both Fe^{2+} and Fe^{3+} states and can possibly occupy one of two crystallographic sites, the large pseudo-dodecahedral Mg site (the A site) or the small octahedral Si site (the B site) (e.g., McCammon 2006; Hsu et al. 2010, 2011). Current consensus on the site occupancy is that Fe^{2+} mainly substitutes for Mg in the A site, whereas Fe^{3+} occupies both the B and A sites. The abundance of Fe^{3+} in the A and B sites appears to depend on the Al content of perovskite. Previous studies have shown that both Fe^{2+} and Fe^{3+} in perovskite exist in the high-spin state under ambient conditions (e.g., McCammon 2006).

Recently, electronic spin states of Fe^{2+} and Fe^{3+} in silicate perovskite have been extensively studied using synchrotron Mössbauer spectroscopy (SMS), X-ray emission spectroscopy (XES), X-ray absorption near-edge spectroscopy (XANES), and by theoretical calculation (e.g., Badro et al. 2004; J. Li et al. 2004, 2006; J. Li 2007; Jackson et al. 2005; L. Li et al. 2005; Zhang and Oganov 2006; Stackhouse et al. 2007; Bengtson et al. 2008, 2009; Lin et al. 2008; McCammon et al. 2008, 2010; Grocholski et al. 2009; Narygina et al. 2009, 2010; Caracas et al. 2010; Catalli et al. 2010; Hsu et al. 2010, 2011; Umemoto et al. 2010). The interpretation of these results has been quite scattered, although there exists a general trend in most Mössbauer studies—both experimental and theoretical studies have reported dominant spectral features with extremely high-quadrupole splitting (QS) values of Fe^{2+} (as high as ~4.4 mm/s) at above ~30 GPa (e.g., Jackson et al. 2005; McCammon et al. 2008; Hsu et al. 2010, 2011; Bengtson et al. 2009). Combined with previous XES analyses for the total spin momentum of iron in perovskite (Badro et al. 2004; Li et al. 2004), the A-site Fe^{2+} with the extremely high QS and relatively high chemical shift (CS) has been interpreted as an occurrence of the intermediate-spin Fe^{2+} with a total spin momentum of one ($S = 1$) (McCammon et al. 2008, 2010; Narygina et al. 2010). That is, a high-spin to intermediate-spin crossover occurs in perovskite at around 30 GPa, and the intermediate-spin Fe^{2+} is predominant in lower-mantle perovskite. The extremely high-QS values of Fe^{2+} have

* E-mail: afu@jsg.utexas.edu

0003-004X/12/0004–592$05.00/DOI: http://dx.doi.org/10.2138/am.2012.4000

also been observed in silicate post-perovskite at lowermost-mantle pressures (Lin et al. 2008; Mao et al. 2010). At higher pressures, the intensity of the extremely high-QS component in perovskite decreases, whereas the intensity of a new component with very low QS of less than 0.5 mm/s and a CS of ~0 mm/s increases. This new component was assigned to the low-spin Fe^{2+} in the A site occurring at 120 GPa and high temperatures (McCammon et al. 2010).

It has been shown, however, that the occurrence of the intermediate-spin state is very rare in geological materials and the high-QS component of iron does not necessarily imply the occurrence of the intermediate-spin state (e.g., Dyar et al. 2006; Bengtson et al. 2009; Hsu et al. 2010, 2011). For example, iron in almandine and majoritic garnet is in the high-spin Fe^{2+} with very high QS of ~3.5 mm/s under ambient conditions (Huggins 1975; Murad and Wagner 1987; Narygina et al. 2010). First-principles theoretical calculations have been recently performed to understand the spin and valence states of iron as well as their associated hyperfine interaction parameters in perovskite at high pressures. Although they are not always in agreement with each other, these calculations show that the intermediate-spin state is not stable at all lower-mantle pressures, irrespective of the exchange-correlation functional used in the calculations (Li et al. 2005; Zhang et al. 2006; Stackhouse et al. 2007; Bengtson et al. 2008, 2009; Caracas et al. 2010; Hsu et al. 2010, 2011; Umemoto et al. 2010). Based on these calculations, the high-spin Fe^{2+} with the QS of 2.3–2.5 mm/s is more stable at relatively low pressures, while the high-spin Fe^{2+} with QS of 3.3–3.6 mm/s is more favorable at higher pressure (Bengtson et al. 2009; Hsu et al. 2010, 2011). The extremely high-QS site is interpreted as a result of the iron atomic-site change, in which iron ions move away from the central positions in the A site at high pressures (Bengtson et al. 2009; Hsu et al. 2010, 2011), rather than the high-spin to the intermediate-spin transition (McCammon et al. 2008; Narygina et al. 2010). The calculations also indicate that anisotropic compressibility is not related to the stabilization of the intermediate state or to the high-spin to the intermediate-spin crossover (Hsu et al. 2010, 2011).

For Fe^{3+} in perovskite, it has been shown both experimentally and theoretically that Fe^{3+} enters into both A and B sites, suggesting a charge-coupled substitution mechanism (e.g., McCammon 1998; Hsu et al. 2011). Combined SMS and XES results for Fe^{3+}-containing perovskite suggest that the low-spin population in the B site gradually increases with pressure up to 50–60 GPa, with all Fe^{3+} in the B site eventually becoming low-spin, though A-site Fe^{3+} remains in the high-spin state to at least 136 GPa, consistent with recent theoretical calculations (Jackson et al. 2005; Catalli et al. 2010; Hsu et al. 2011). That is, Fe^{3+} in the octahedral B site undergoes a high-spin to low-spin transition in perovskite at high pressures. SMS analyses further suggest that Fe^{3+} in the A site remains in the high-spin state in Al-bearing perovskite in, which Fe^{3+} is expected to predominantly exist in the A site (Grocholski et al. 2009; Catalli et al. 2010).

These recent experimental studies have mostly relied on Mössbauer spectroscopic results, which have proven very effective in studying iron-bearing minerals in the past. There is a large body of evidence pointing out the relationship between measured hyperfine interaction parameters and valence, spin, and magnetic states of iron and its compounds at ambient and under extreme conditions. However, because of the complex crystal chemistry in perovskite, experimental results and their interpretations have been quite difficult. For example, some of the experiments were conducted using uncharacterized samples under non-hydrostatic conditions without the use of an inert pressure medium at high pressures, which could result in an investigation of the sample's amorphous state as perosvkite is a relatively unstable phase after being quenched to ambient conditions. On the other hand, the use of the Fe_2O_3-containing $MgSiO_3$ glass to synthesize Fe^{3+}-containing perovskite has been shown to produce a Fe_2O_3 impurity that coexists with the sample (Catalli et al. 2010), which can contaminate Mössbauer spectra and hence the interpretation of the results. To provide new insight on the spin and valence states of iron in lower-mantle perovskite, we have performed high-pressure SMS experiments with a well-characterized starting perovskite sample in a quasi-hydrostatic Ne pressure medium. These results allow us to identify the high-spin to low-spin transition of Fe^{3+} in the B site occurring between ~13 and 24 GPa. The spin pairing of the B-site Fe^{3+} occurs simultaneously with two extremely high-QS doublets of the dodecahedral-site Fe^{2+}. Our results thus reconcile recent experimental and theoretical studies on the spin and valence states of iron and hyperfine interaction parameters in lower-mantle perovskite at high pressures.

Experimental methods

^{57}Fe-enriched enstatite powder [$(Mg_{0.9},Fe_{0.1})SiO_3$] was used as the starting sample for synthesizing silicate perovskite. The enstatite powder was synthesized by mixing powders of the oxides SiO_2, MgO, and $^{57}Fe_2O_3$ (90% enrichment or better) in the appropriate ratios, which were then heated in a gas-mixing furnace with CO and CO_2 gases at 1295 °C and an oxygen fugacity 1.6 log units below the nickel-nickel oxide buffer. Mössbauer analyses of the enstatite powder showed two doublets, which can be assigned to the high-spin Fe^{2+} in the M1 and M2 sites; there was no evidence for Fe^{3+} within the detection limit of ~3% $Fe^{3+}/\Sigma Fe$. The enstatite powder was placed in a dry oven at 160 °C and then loaded into an AuPd capsule for high-pressure-temperature experiments in the Orange-3000 ton multi-anvil press at the Geodynamic Research Center (GRC), Ehime University. The sample assemblage was compressed to about 23–24 GPa with all the available loading pressure of the press, and a Pt heater was used to heat the sample to 1400 °C for an hour. The quenched sample was analyzed by electron microscope, X-ray diffraction, and Mössbauer spectroscopies. Electron microscope analyses showed that the synthesized sample had a chemical composition of $(Mg_{0.9},Fe_{0.1})SiO_3$. The angle-dispersive X-ray diffraction pattern of the synthesized sample was dominated by the silicate perovskite structure (*Pbnm*) (Fig. 1). However, ~10% of stishovite (SiO_2) was also detected, suggesting a small loss of (Mg,Fe)O ferropericlase to the capsule during sample syntheses. The coexistence of stishovite and perovskite is not expected to contaminate the SMS spectra as iron solubility in stishovite is known to be negligible. The refined cell parameters of the perovskite are: a = 4.7981 (±0.0002), b = 4.9447 (±0.0002), and c = 6.9231 (±0.0003) Å, consistent with previous studies (e.g., McCammon 2006; McCammon et al. 2008).

A traditional Mössbauer spectrum of the synthesized perovskite was recorded at room temperature and pressure in transmission mode on a constant acceleration Mössbauer spectrometer with a nominal 370 MBq ^{57}Co high-specific activity source in a 12 μm thick Rh matrix at the Bayerisches Geoinstitut, Universität Bayreuth (McCammon 2006) (Fig. 2). The spectrum, collected over 3 days, was fitted using the commercially available fitting program NORMOS written by R.A. Brand (distributed by Wissenschaftliche Elektronik GmbH, Germany) (Fig. 2). The Mössbauer spectrum was similar to those in the literature for silicate perovskite and was fitted to three Lorentzian doublets using conventional constraints (i.e., equal areas and widths of components). Analysis of the Mössbauer spectrum shows three doublets, two assigned to Fe^{2+} and one to Fe^{3+}, in the perovskite structure. The relative areas were corrected for differences in recoil-free fraction between Fe^{2+} and Fe^{3+} in the perovskite structure (McCammon 1998), and trial fits were made using the full transmission integral to account for thickness effects. The derived

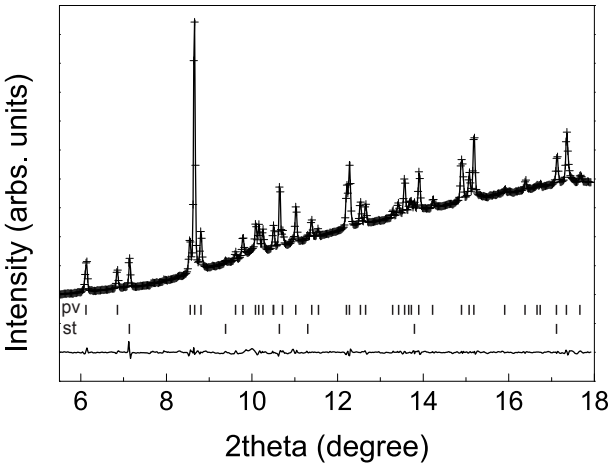

FIGURE 1. Representative X-ray diffraction pattern of the synthesized silicate perovskite sample. Full-profile Rietveld refinement of the spectrum showed that the sample was in the *Pbnm* perovskite structure. A small amount of stishovite (~10%, which is labeled st) is also detected in the pattern. The refined cell parameters are: a = 4.7981 (±0.0002), b = 4.9447 (±0.0002), c = 6.9231 (±0.0003) Å. The wavelength of the X-ray source was 0.368 Å.

hyperfine parameters (mm/s) are as follows: two Fe^{2+} doublets with QS = 1.54 (±0.02) and CS = 1.11 (±0.01), and QS = 1.97 (±0.08) and CS = 1.12 (±0.02); and one Fe^{3+} doublet with QS = 0.89 (±0.04) and CS = 0.43 (±0.02). The derived Fe^{3+} content ($Fe^{3+}/\sum Fe$) in the analyses is ~25–30%. There is no evidence for metallic Fe, but fits were made by incorporating a sextet, which enabled a detection limit of ~4% of the relative area for the total amount of iron in the sample to be estimated.

The synthesized sample was polished to a flat disk 12 µm thick and 40 µm in diameter. A rhenium gasket was pre-indented by a pair of beveled diamond anvils having 300 µm outer culet and 150 µm inner culet to a thickness of 25 µm. A hole of 90 µm in diameter was drilled in the pre-indented gasket and used as the sample chamber. The sample disk was then loaded into the sample chamber of a diamond-anvil cell (DAC), with a neon pressure medium and a few ruby spheres for pressure calibration in a high-pressure gas loader. Before the gas loading, the high-pressure gas loading system was evacuated for 30 min to prevent any air or moisture contamination. The double-polished sample disk with a homogeneous thickness ensured less distortion of the SMS spectra from the thickness effect of the sample, whereas the use of the Ne medium and a small X-ray beam allowed SMS spectra to be taken from the sample with a much smaller pressure gradient.

SMS experiments were carried out at the undulator beamline 3-IDB and 16-IDD of the Advanced Photon Source (APS), Argonne National Laboratory (ANL) (Sturhahn 2000). A monochromatic X-ray beam of ~14.4125 keV with 153.4 ns separation between the individual bunches and 1 meV resolution at 3-ID and 2 meV resolution at 16-IDD was used to excite the nuclear resonance of the ^{57}Fe nuclei in the sample. The focused X-ray beam was ~7 µm in diameter at 3-IDB and 20 µm in diameter at 16-IDD, where a cleanup slit of 20 µm in diameter was used to remove the unwanted tail of the focused X-ray beam. The very small X-ray beam size significantly reduced the influence of the pressure gradients in the radial direction across the sample chamber. The time-delayed spectra were recorded by an avalanche photodiode detector (APD) in the forward direction. The data collection time for each SMS spectrum was ~3 to 4 h. Pressures were measured using the ruby R_1 luminescence peak of the ruby sphere placed next to the sample (Mao et al. 1978), whereas X-ray diffraction patterns were taken from the sample at high pressures to confirm that the sample remained in the perovskite structure.

EXPERIMENTAL RESULTS

The SMS spectra of the sample were collected up to 120 GPa (Fig. 3). The Mössbauer spectral features below ~13 GPa were dominated by a broad time beat similar to previous studies on Al-free perovskite (Jackson et al. 2005; McCammon et al. 2008). The spectral features started to change significantly between 13 and 36 GPa, at which point more time beats were observed. Above 36 GPa, the spectra are dominated by five time beats with very narrow time widths, indicating the occurrence of the higher QS components in the sample. These observations suggest a transition in the hyperfine parameters of the iron sites between 13 and 36 GPa.

The spectra were evaluated with the CONUSS program to derive the hyperfine parameters, QS, and relative CS, at high pressures (Sturhahn 2000). Based on traditional Mössbauer analyses at ambient conditions (Fig. 2) and previous studies (Jackson et al. 2005; McCammon et al. 2008), the spectra below 20 GPa were adequately fitted with a three-doublet model, whereas a fourth doublet was needed to satisfactorily explain the spectral features above 24 GPa (Figs. 4 and 5). Corresponding energy spectra were then calculated from the fits using the CONUSS program (Sturhahn 2000). Based on the three-doublet model using the CONUSS program, the derived QS values and relative abundances of the doublets at ambient conditions are consistent with the traditional Mössbauer analyses of the sample (Figs. 2–5). These spectral evaluations likely carry uncertainties in the order of ±5% for the derived hyperfine parameters and site abundances, although the uncertainties are likely larger (~10%) in the transition region between 13 to 36 GPa.

DISCUSSION

Based on literature values and our derived hyperfine parameters (Fig. 6) (Jackson et al. 2005; McCammon et al. 2008; Bengtson et al. 2009; Grocholski et al. 2009; Catalli et al. 2010; Hsu et al. 2010, 2011; Narygina et al. 2010), doublets 1 and 2 can be associated with the high-spin Fe^{2+} in the A site at ambient pressure (Figs. 4–6), whereas doublet 3, with an extremely low QS of 0.65 mm/s and an abundance of ~20–25%, can be assigned to high-spin Fe^{3+}. The assigned amount of Fe^{3+} in the sample is consistent with traditional Mössbauer analyses under ambient conditions (Fig. 2). At ambient conditions, doublet 1,

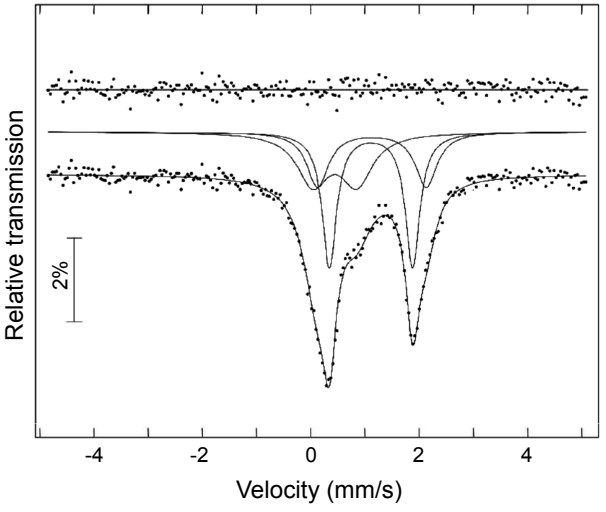

FIGURE 2. Ambient-condition Mössbauer spectrum of the synthesized ^{57}Fe-enriched $(Mg_{0.9},Fe_{0.1})SiO_3$ silicate perovskite. The spectrum was fitted with a three-doublet model, two assigned to Fe^{2+} in the A site and one to Fe^{3+}. The amount of Fe^{3+} was determined based on the relative areas corrected for different recoil-free fractions of Fe^{2+} and Fe^{3+}, and was found to be 25–30% of the total Fe content.

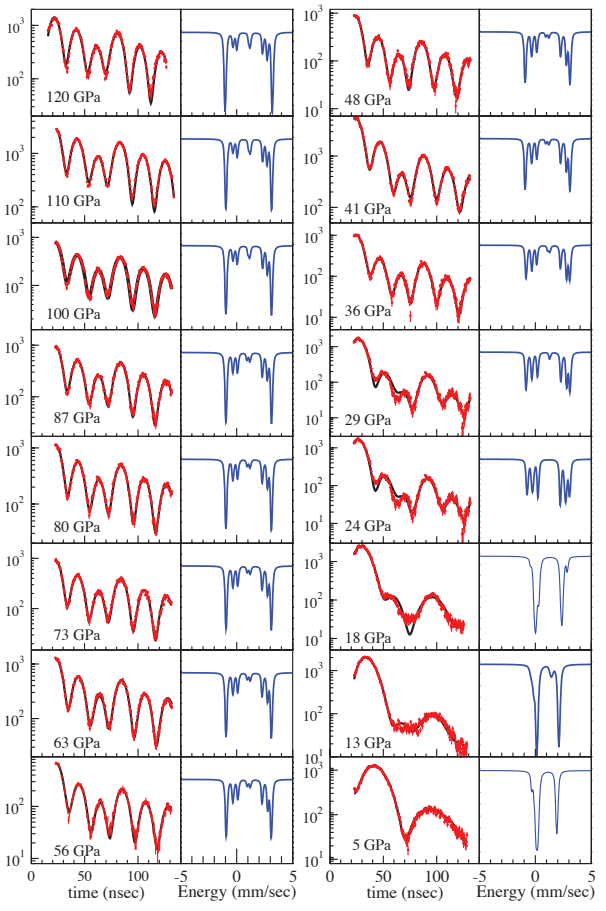

FIGURE 3. Representative synchrotron Mössbauer spectra of $(Mg_{0.9},Fe_{0.1})SiO_3$ silicate perovskite at high pressures. Corresponding energy spectra calculated from the fits are shown in the right panels (blue lines). Red dots: experimental SMS spectra; black lines: modeled spectra. The spectra were fitted to three iron doublets at 0, 5, 13, and 18 GPa, whereas a four-doublet model was used starting at 24 GPa. The derived QS values are plotted in Figure 4. (Color online.)

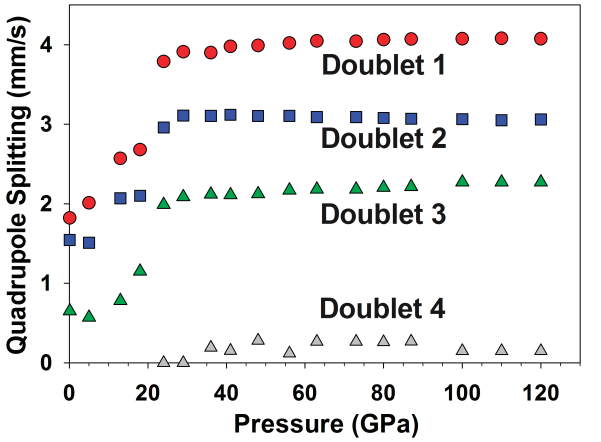

FIGURE 4. Derived quadrupole splitting (QS) of iron in $(Mg_{0.9},Fe_{0.1})SiO_3$ silicate perovskite at high pressures and 300 K. (Color online.)

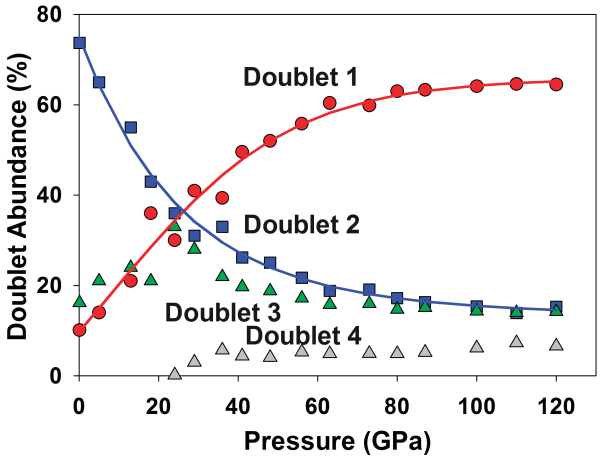

FIGURE 5. Relative doublet abundances of iron in perovskite at high pressures and 300 K. Doublets 1 and 2 are assigned to be high-spin Fe^{2+} in the A site. Curves associated with these doublets are shown to allow readers to follow their trends. Doublet 3 represents Fe^{3+}, which undergoes a high-spin to low-spin transition at ~13–24 GPa, whereas doublet 4 represents residual, untransformed high-spin Fe^{3+} in the A site. (Color online.)

with an abundance of 11% and a QS of 1.82 mm/s, is much less abundant than doublet 2, with an abundance of 74% and a QS of 1.54 mm/s. These two doublets account for ~75–80% abundance of all iron sites.

It should be noted that the QS of the iron site arises from the interaction between the nuclear quadrupole moment and the non-spherical component of the electronic charge distribution described by its effective electric-field gradient (EFG) in a simplified model (Maddock 1997; Dyar et al. 2006). In general, the electric-field gradient in the vicinity of the ^{57}Fe nucleus can be attributed to a lattice contribution from the crystal field produced by the surrounding ions and an electronic contribution from the non-spherical charge distribution of the electron shell surrounding the nucleus (Maddock 1997; Dyar et al. 2006). That is, the conversion of doublet 2 to doublet 1, as a function of pressure, can be attributed to the pressure-induced lattice distortion and enhanced effective electric-field gradient in the A site of the high-spin Fe^{2+} (McCammon et al. 2008) (Figs. 4 and 5). On the other hand, the QS and the 20–25% abundance of the doublet 3 assigned to the high-spin Fe^{3+} are not affected by increasing pressure up to 13 GPa, but start to change dramatically above 13–18 GPa (Figs. 4 and 5). We note that high-spin Fe^{3+} is known to exhibit very low QS compared to Fe^{2+} because all five 3*d* electrons are unpaired and form relatively spherical electronic orbitals. Since high-spin Fe^{3+} shows very low QS in both the A and B sites (Fig. 6), it is rather difficult to distinguish its coordination from the QS values alone.

We have used a four-doublet model to adequately explain the spectral features starting at 24 GPa. The increase in abundance of doublet 1 with a QS of 3.8–4.1 mm/s is associated with decreasing abundance of doublet 2 with a QS of 3.0–3.1 mm/s above 13–18 GPa (Figs. 4 and 5). Although further increasing pressure appears to have a minimum effect on increasing the QS values, the abundance of doublet 1 increases with pressure concurrently

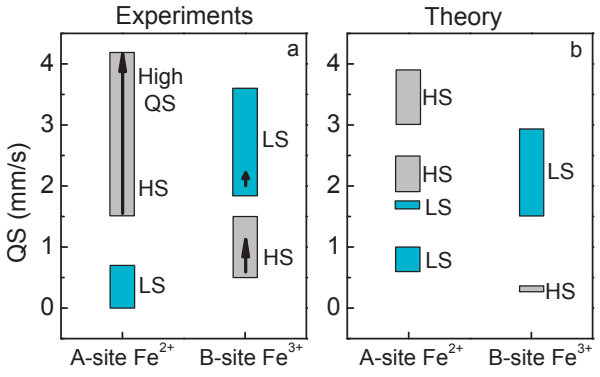

FIGURE 6. Quadrupole splitting (QS) of Fe in perovskite from recent experimental (**left**) and theoretical (**right**) results (Li et al. 2006; Jackson et al. 2005; Lin et al. 2008; McCammon et al. 2008, 2010; Bengtson et al. 2009; Grocholski et al. 2009; Narygina et al. 2009, 2010; Catalli et al. 2010; Hsu et al. 2010, 2011). Black arrows show the effect of increasing pressure on the QS values from this study. A and B represent two different crystallographic sites of Fe in perovskite. (Color online.)

and continuously with a decrease in the abundance of doublet 2 (Fig. 4). That is, more Fe^{2+} has exhibited extremely high QS of ~4.1 mm/s at higher pressures. Based on a total abundance of 20–25% and relatively low-QS values, doublets 3 and 4 at pressures above 24 GPa can be associated with doublet 3 of the high-spin Fe^{3+} at ambient conditions. The QS of doublet 3 jumps dramatically from 0.65 to 2 mm/s between 13 and 24 GPa, while doublet 4, with an abundance of ~5%, exhibits a very small QS of ~0.2 mm/s. Their total abundance and individual QS values are, however, not significantly influenced by further pressure increase (Figs. 4–6).

Based on the behavior of the derived hyperfine parameters and associated doublet abundances, we provide here a coherent model to explain our observations, which are consistent with previous theoretical and experimental results (Fig. 6). The dramatic increase in the QS of doublet 3 can be explained as a result of the high-spin to low-spin transition of Fe^{3+} in the B site between 13 and 24 GPa, which is believed to be accompanied by a noticeable volume reduction in the unit cell of perovskite (Catalli et al. 2010; Hsu et al. 2011). Based on crystal field theory and recent first-principles theoretical calculations, the high-spin Fe^{3+} in the octahedral site has five 3*d* electrons that spherically occupy all five e_g and t_{2g}-like orbitals, each with relatively longer Fe-O bond lengths; low-spin 3*d* electrons of the B-site iron only occupy the non-spherical t_{2g}-like orbitals hybridized with the surrounding oxygen ions with reduced Fe-O distances (Burns 1993; Hsu et al. 2011). With increasing pressure, the internal octahedral bond lengths can be shortened enough to induce the spin-pairing crossover of Fe^{3+}. The high-spin to low-spin transition in the B-site Fe^{3+} results in a significant increase in the effective electric field gradient and thus the QS. Such increase in the QS across the spin-pairing transition has also been observed in the rare-earth orthoferrite perovskites ($LaFeO_3$ and $PrFeO_3$), which have the same perovskite structure (Xu et al. 2001; Rozenberg et al. 2005). On the other hand, doublet 4 with very low QS can be assigned to the high-spin Fe^{3+} in the A site. Residing in the large dodecahedral cage, the A-site Fe^{3+} can easily maintain longer Fe-O distances and remains in the high-spin state up to 120 GPa, consistent with recent theoretical and experimental observations (Catalli et al. 2010; Hsu et al. 2011). This doublet is originally indistinguishable in the QS value from the high-spin Fe^{3+} in the B site, but becomes distinctive from the B-site low-spin Fe^{3+} across the spin transition (Fig. 6). Theoretical calculations further suggest that the high-spin Fe^{3+} in the A site has a slightly lower QS value than the high-spin Fe^{3+} in the B site, whereas the low-spin Fe^{3+} in the A site should have a much higher QS as well (Hsu et al. 2010, 2011) (Fig. 6). Based on our model, about half of the total Fe^{3+} should occupy the lattice through charge-coupled substitutions in the A and B sites ($Mg_A^{2+} + Si_B^{4+} \rightarrow Fe_B^{3+} + Fe_A^{3+}$) (subscripts denote crystallographic sites) (McCammon 1998; Catalli et al. 2010; Hsu et al. 2011), whereas another half of the total Fe^{3+} would exist in the lattice through oxygen vacancy substitutions

$$Si_B^{4+} + \frac{1}{2}O^{2-} \rightarrow Fe_B^{3+} + \frac{1}{2}V_O^0$$

where V denotes an oxygen vacancy (Navrotsky et al. 2003).

Based on the dramatic increase in the QS values and subsequent redistribution of the A-site Fe^{2+} abundance, it is conceivable that the occurrence of the extremely high-QS values are related to the high-spin to low-spin transition of the Fe^{3+} in the B site at 13–36 GPa. Similar to ferropericlase at high pressures (Lin et al. 2005; Tsuchiya et al. 2006), the spin transition of the B-site Fe^{3+} in perovskite results in a noticeable volume reduction through the 3*d* electronic configurations and shortened Fe-O distances in the octahedral sites (Catalli et al. 2010; Hsu et al. 2011), which in turn can change the local structural geometries, the iron atomic positions, and the bond lengths and angles of the A-site Fe^{2+}. Such changes can be manifested in the dramatic increase of the QS values and the redistribution of the site abundance in doublets 1 and 2 associated with the A-site Fe^{2+}. As pressure increases further, the A-site Fe^{2+} with relatively low QS is continuously converted to doublet 1 component with extremely high QS. That is, the spin-pairing transition of the octahedral-site Fe^{3+} causes a volume reduction and a change in the local atomic-site configurations that can result in the significant increase of the quadrupole splitting in the dodecahedral-site Fe^{2+} at 13–24 GPa. The observed spin transition in the B-site Fe^{3+} can also help elucidate the partial reduction in the total spin momentum observed in previous XES studies (Badro et al. 2004; Li et al. 2004).

Since theoretical predictions indicate that the spin-pairing transition causes a softening in the bulk modulus and bulk sound velocity of Fe^{3+}-containing perovskite, it remains to be further understood as to how the spin-pairing transition affects our understanding of the geophysics and geochemistry of the lower mantle.

Since Earth's lower mantle is subject to pressures ranging from 23 to 136 GPa and high temperatures, low-spin Fe^{3+} likely becomes more stable in perovskite at lower-mantle conditions. The site abundance of the Fe^{3+} in the A and B sites thus indicates that both charge-coupled substitution and oxygen vacancy substitution mechanisms proposed previously play equally important roles in the crystal chemistry of Fe^{3+} in the Al-free perovskite lattice. The spin-pairing transition of Fe^{3+} results in a volume

reduction of the octahedral site (Catalli et al. 2010; Hsu et al. 2011), which then concurrently affects the lattice geometry and atomic site position of the high-spin A-site Fe^{2+} in perovskite. One can thus associate the dramatic increase in the extremely high-QS doublets of the A-site Fe^{2+} to the spin-pairing transition of the B-site Fe^{3+}. Since theoretical predictions indicate that the spin-pairing transition causes a softening in the bulk modulus and bulk sound velocity of Fe^{3+}-containing perovskite, it remains to be further understood as to how the spin-pairing transition affects our understanding of the geophysics and geochemistry of the lower mantle.

Acknowledgments

High-pressure experiments were performed at XOR3, HPCAT, and GSECARS of the Advanced Photon Source (APS) at the Argonne National Laboratory (ANL). HPCAT is supported by DOE-BES, DOE-NNSA, NSF, and the W.M. Keck Foundation. APS is supported by DOE-BES, under contract no. DE-AC02-06CH11357. J.F.L. and Z.M. acknowledge support from the U.S. National Science Foundation (EAR-0838221 and EAR-1056670), Energy Frontier Research Centers (EFRCs), and the Carnegie/DOE Alliance Center (CDAC). We also thank H. Hsu and S. Speziale for helpful discussions and A. Wheat for editing the manuscript.

References cited

Badro, J., Rueff, J.P., Vankó, G., Monaco, G., Fiquet, G., and Guyot, F. (2004) Electronic transitions in perovskite: possible nonconvecting layers in the lower mantle. Science, 305, 383–386.

Bengtson, A., Persson, K., and Morgan, D. (2008) Ab initio study of the composition dependence of the pressure-induced spin crossover in perovskite $(Mg_{1-x},Fe_x)SiO_3$. Earth and Planetary Science Letters, 265, 535–545.

Bengtson, A., Li, J., and Morgan, D. (2009) Mössbauer modeling to interpret the spin state of iron in $(Mg,Fe)SiO_3$ perovskite. Geophysical Research Letters, 36, L15301.

Burns, R.G. (1993) Mineralogical applications of crystal field theory. Cambridge University Press, U.K.

Caracas, R., Mainprice, D., and Thomas, C. (2010) Is the spin transition in Fe^{2+}-bearing perovskite visible in seismology? Geophysical Research Letters, 37, L13309.

Catalli, K., Shim, S.-H., Prakapenka, V.B., Zhao, J., Sturhahn, W., Chow, P., Xiao, Y., Liu, H., Cynn, H., and Evans, W.J. (2010) Spin state of ferric iron in $MgSiO_3$ perovskite and its effect on elastic properties. Earth and Planetary Science Letters, 289, 68–75.

Dyar, M.D., Agresti, D.G., Schaefer, M.W., Grant, C.A., and Sklute, E.C. (2006) Mössbauer spectroscopy of Earth and planetary materials. The Annual Review of Earth and Planetary Sciences, 34, 83–125.

Grocholski, B., Shim, S.-H., Sturhahn, W., Zhao, J., Xiao, Y., and Chow, C. (2009) Spin and valence states of iron in $(Mg_{0.8}Fe_{0.2})SiO_3$ perovskite. Geophysical Research Letters, 36, L24303.

Hsu, H., Umemoto, K., Blaha, P., and Wentzcovitch, R.M. (2010) Spin states and hyperfine interactions of iron in $(Mg,Fe)SiO_3$ perovskite under pressure. Earth and Planetary Science Letters, 294, 19–26.

Hsu, H., Blaha, P., Cococcioni, M., and Wentzcovitch, R.M. (2011) Spin-state crossover and hyperfine interactions of ferric iron in $MgSiO_3$ perovskite. Physical Review Letters, 106, 118501.

Huggins, F.E. (1975) The 3*d* levels of ferrous ions in silicate garnets. American Mineralogist, 60, 316–319.

Jackson, J.M., Sturhahn, W., Shen, G., Zhao, J., Hu, M.Y., Errandonea, D., Bass, J.D., and Fei, Y. (2005) A synchrotron Mössbauer spectroscopy study of $(Mg,Fe)SiO_3$ perovskite up to 120 GPa. American Mineralogist, 90, 199–205.

Li, J. (2007) Electronic transitions and spin states in perovskite and post-perovskite. In K. Hirose, J. Brodholt, T. Lay, and D. Yuen, Eds., Post-Perovskite: The Last Mantle Phase Transition, p. 47–69. American Geophysical Union, Washington, D.C.

Li, J., Struzhkin, V., Mao, H.K., Shu, J., Hemley, R., Fei, Y., Mysen, B., Dera, P., Prakapenka, V., and Shen, G. (2004) Electronic spin state of iron in lower mantle perovskite. Proceedings of the National Academy of Sciences, 101, 14027–14030.

Li, J., Sturhahn, W., Jackson, J.M., Struzhkin, V.V., Lin, J.F., Zhao, J., Mao, H.K., and Shen, G. (2006) Pressure effect on the electronic structure of iron in $(Mg,Fe)(Al,Si)O_3$ perovskite: A combined synchrotron Mössbauer and X-ray emission spectroscopy study up to 100 GPa. Physics and Chemistry of Minerals, 33, 575–585.

Li, L., Brodholt, J.P., Stackhouse, S., Weidner, D.J., Alfredsson, M., and Price, G.D. (2005) Electronic spin state of ferric iron in Al-bearing perovskite in the lower mantle. Geophysical Research Letters, 32, L17307.

Lin, J.F. and Tsuchiya, T. (2008) Spin transition of iron in the Earth's lower mantle. Physics of the Earth and Planetary Interiors, 170, 248–259.

Lin, J.F., Struzhkin, V.V., Jacobsen, S.D., Hu, M., Chow, P., Kung, J., Liu, H., Mao, H.K., and Hemley, R.J. (2005) Spin transition of iron in magnesiowüstite in Earth's lower mantle. Nature, 436, 377–380.

Lin, J.F., Watson, H.C., Vankó, G., Alp, E.E., Prakapenka, V.B., Dera, P., Struzhkin, V.V., Kubo, A., Zhao, J., McCammon, C., and Evans, W.J. (2008) Intermediate-spin ferrous iron in lowermost mantle post-perovskite and perovskite. Nature Geoscience, 1, 688–691.

Maddock, A.G. (1997) Mössbauer spectroscopy: Principles and applications of the techniques, p. 258. Albion/Horwoord Publishing, Chichester.

Mao, H.K., Bell, P.M., Shaner, J.W., and Steinberg, D.J. (1978) Specific volume measurements of Cu, Mo, Pd, and Ag and calibration of the ruby R_1 fluorescence pressure gauge from 0.06 to 1 Mbar. Journal of Applied Physics, 49, 3276–3287.

Mao, Z., Lin, J.F., Jacobs, C., Watson, H., Xiao, Y., Chow, P., Alp, E.E., and Prakapenka, V.B. (2010) Electronic spin and valence states of Fe in CaIrO3-type post-perovskite in the Earth's lowermost mantle. Geophysical Research Letters, 37, L22304.

McCammon, C. (1997) Perovskite as a possible sink for ferric iron in the lower mantle. Nature, 387, 694–696.

——— (1998) The crystal chemistry of ferric iron in $Fe_{0.05}Mg_{0.95}SiO_3$ perovskite as determined by Mössbauer spectroscopy in the temperature range 80-293 K. Physics and Chemistry of Minerals, 25, 292–300.

——— (2006) Microscopic properties to macroscopic behavior: The influence of iron electronic state. Journal of Mineralogical and Petrological Sciences, 101, 130–144.

McCammon, C., Kantor, I., Narygina, O., Rouquette, J., Ponkratz, U., Sergueev, I., Mezouar, M., Prakapenka, V., and Dubrovinsky, L. (2008) Intermediate-spin ferrous iron in lower mantle perovskite. Nature Geoscience, 1, 684–687.

McCammon, C., Dubrovinsky, L., Narygina, O., Kantor, I., Wu, X., Glazyrin, K., Sergueev, I., and Chumakov, A.I. (2010) Low-spin Fe^{2+} in silicate perovskite and a possible layer at the base of the lower mantle. Physics of the Earth and Planetary Interiors, 180, 215–221.

Murad, E. and Wagner, F.E. (1987) The Mössbauer spectrum of almandine. Physics and Chemistry of Minerals, 14, 264–269.

Narygina, O., Mattesini, M., Kantor, I., Pascarelli, S., Wu, X., Aquilanti, G., McCammon, C., and Dubrovinsky, L. (2009) High-pressure experimental and computational XANES studies of $(Mg,Fe)(Si,Al)O_3$ perovskite and (Mg,Fe)O ferropericlase as in the Earth's lower mantle. Physical Review B, 79, 174115.

Narygina, O.V., Kantor, I.Y., McCammon, C.A., and Dubrovinsky, L.S. (2010) Electronic state of Fe^{2+} in $(Mg,Fe)(Si,Al)O_3$ perovskite and $(Mg,Fe)SiO_3$ majorite at pressures up to 81 GPa and temperatures up to 800 K. Physics and Chemistry of Minerals, 37, 407–415.

Navrotsky, A., Schoenitz, M., Kojitani, H., Xu, H.W., Zhang, J.Z., Weidner, D.J., and Jeanloz, R. (2003) Aluminum in magnesium silicate perovskite: formation, structure, and energetics of magnesium-rich defect solid solutions. Journal of Geophysical Research, 108, 2330.

Ringwood, A.E. (1982) Phase transformations and differentiation in subducted lithosphere: implications for mantle dynamics basalt petrogenesis and crustal evolution. Journal of Geology, 90, 611–642.

Rozenberg, G., Pasternak, M., Xu, W., Dubrovinsky, L., Carlson, S., and Taylor, R. (2005) Consequences of pressure-instigated spin crossover in RFeO3 perovskites; a volume collapse with no symmetry modification. Europhysics Letters, 71, 228–234.

Stackhouse, S., Brodholt, J.P., and Price, G.D. (2007) Electronic spin transitions in iron-bearing $MgSiO_3$ perovskite. Earth and Planetary Science Letters, 253, 282–290.

Sturhahn, W. (2000) CONUSS and PHOENIX: Evaluation of nuclear resonant scattering data. Journal of Physics: Condensed Matter, 16, 149–172.

Tsuchiya, T., Wentzcovitch, R.M., da Silva, C.R.S., and de Gironcoli, S. (2006) Spin transition in magnesiowüstite in Earth's lower mantle. Physical Review Letters, 96, 198501.

Umemoto, K., Hsu, H., and Wentzcovitch, R.M. (2010) Effect of site degeneracies on the spin crossovers in $(Mg,Fe)SiO_3$ perovskite. Physics of the Earth and Planetary Interiors, 180, 209–214.

Xu, W.M., Naaman, O., Rozenberg, G., Pasternak, M.P., and Taylor, R.D. (2001) Pressure-induced breakdown of a correlated system: the progressive collapse of the Mott-Hubbard state of $RFeO_3$. Physical Review B, 64, 094411.

Zhang, F. and Oganov, A.R. (2006) Valence state and spin transitions of iron in Earth's mantle silicates. Earth and Planetary Science Letters, 249, 436–443.

Manuscript received September 9, 2011
Manuscript accepted December 9, 2011
Manuscript handled by Sergio Speziale